Macromolecules

Article

pubs.acs.org/Macromolecules

Formation of Lenticular Platelet Micelles via the Interplay of Crystallization and Chain Stretching: Solution Self-Assembly of Poly(ferrocenyldimethylsilane)-*block*-poly(2-vinylpyridine) with a Crystallizable Core-Forming Metalloblock

Siti Fairus Mohd Yusoff,[†,‡] Ming-Siao Hsiao,[†] Felix H. Schacher,[†,⊥] Mitchell A. Winnik,*[,§] and Ian Manners*[,†]

[†]School of Chemistry, University of Bristol, Bristol BS8 1TS, U.K.

[‡]Universiti Kebangsaan Malaysia, 43600 UKM Bangi, Selangor, Malaysia

[§]Department of Chemistry, University of Toronto, 80 St. George Street, Toronto, Ontario, Canada M5S 3H6

Supporting Information

ABSTRACT: The influence of solvent composition on micelle morphology has been investigated for two crystalline-coil poly(ferrocenyldimethylsilane-*block*-2-vinylpyridine) (PFS-*b*-P2VP) diblock copolymers with different block ratios (5:1 and 1:1). The solution self-assembly of these materials was explored in solvent mixtures containing different ratios of a good solvent for both blocks (THF) and a selective solvent for the P2VP block (isopropanol). Various micellar morphologies such as spheres and platelets were characterized using transmission electron microscopy (TEM), selected area electron diffraction (SAED), dynamic light scattering (DLS), wide-angle X-ray scattering (WAXS), and atomic force microscopy (AFM). The results showed that the solution self-assembly of PFS-*b*-P2VP block copolymers (5:1, 1:1) gave spherical micelles with an amorphous PFS core at low THF content (10 vol %). Subsequently, the amorphous spheres were slowly transformed into platelet micelles with a lenticular shape that consisted of a crystalline PFS core sandwiched by two coronal P2VP layers. This indicated that the amorphous spherical micelles were in a metastable state. The transformation of spheres into platelets was significantly slower for the 5:1 block copolymer with the longer PFS core-forming segment presumably due to a lower rate of crystallization of the metalloblock. Platelets were found to be dominant for both block copolymers at higher THF content (THF ≥ 30 vol %). The formation of lenticular rather than regular platelets was attributed to a poisoning effect whereby interference of the P2VP corona-forming blocks in the growth of the crystalline PFS core leads to the creation of defects in the crystal growth fronts.

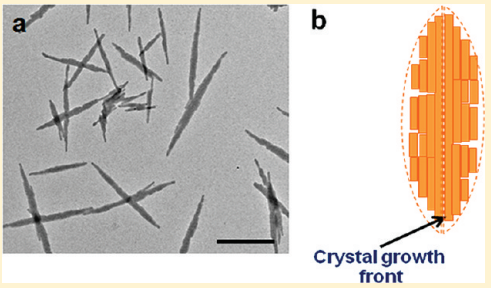

INTRODUCTION

Block copolymers have received considerable attention due to their ability to self-assemble into a variety of different morphologies either in bulk or in solution.[1−3] In the bulk state, block copolymers form ordered arrays of nanostructures as a result of the inherent immiscibility of the constituent blocks.[4,5] When dissolved in a block selective solvent, block copolymers can self-assemble to form various micellar aggregates such as spheres,[6,7] cylinders,[8,9] and more complex architectures.[6,10,11] It is known that several parameters influence the equilibrium morphologies in the solution state.[12,13] These parameters include the stretching of the core-forming block, intercoronal chain repulsions, and the interfacial free energy between the solvent and the micellar core. Hence, transformations between different micellar morphologies can be induced via changes in the block ratio or the solvent characteristics.[12,14−16]

The influence of the crystallization on the self-assembly of diblock copolymers in solution was initially explored in the mid-1960s[17] and has attracted growing attention over the past decade as a method for morphology control, the preparation of functional nanostructures, and the formation of hierarchical architectures by epitaxial growth processes.[1,18,19] It has been well-established in both early and more recent in depth studies that for crystalline-coil diblock copolymers such as poly(ethylene oxide)-*b*-polystyrene (PEO-*b*-PS), if the chosen solvent was a theta or poor solvent for the crystalline block but a selective solvent for the coil block, thin sandwiched lamellar diblock copolymer single crystals consisting of a chain folded polymer single crystal and two covered coil layers were formed.[17,20,21a,22−24]

We have been particularly interested in the solution self-assembly of metal-containing polyferrocenylsilane (PFS)-based crystalline-coil diblock copolymers.[1] Below the melting temper-

Received: December 22, 2011
Revised: March 15, 2012
Published: April 26, 2012

ature of the PFS block in a selective solvent for the coil block, these materials tend to form elongated cylindrical or platelet micelles depending on the block ratio.[21] It has been shown that the formation of these two morphologies is driven by the crystallization of the PFS core.[8,21] The formation of the cylindrical micelles or lamellar structures (platelets) is governed by the interplay between crystallization of the PFS core, which favors extended crystalline lamellar platelets, and the stretching of the amorphous coronal block, which forces the core−coronal interface to curve and thereby confines the lateral extent of the platelets.[21]

We have previously reported the self-assembly behavior of asymmetric PFS-*b*-P2VP block copolymers with a long P2VP block (block ratios; 1:7 and 1:10) in various alcohols, which are selective solvents for the P2VP block.[7,14] Our studies showed that cylindrical micelles with a crystalline PFS core are the dominant morphology in isopropanol (*i*PrOH), whereas spheres with an amorphous PFS core form in methanol. In ethanol, spherical micelles were also found to form initially, but over several weeks, a micellar sphere-to-cylinder transition was detected.[7,14] These studies indicated that by adjusting the solvent quality for the hydrophobic PFS core-forming block, it is possible to influence the ability of this segment to crystallize and thereby to trap metastable micelle morphologies and to induce morphological changes. As a complement to this work on asymmetric materials, in this paper we describe detailed studies of the self-assembly behavior of PFS-*b*-P2VP block copolymers where the crystallizable PFS core possesses an equal or greater degree of polymerization compared to the P2VP coronal-forming segment. A THF/isopropanol (*i*PrOH) mixed solvent system was chosen for this study as THF is a common solvent for both blocks while *i*PrOH is a selective solvent for the P2VP block. Specifically, we have studied the evolution of the micellar morphology and the final structures formed for two PFS-*b*-P2VP block copolymers with different block ratios of 1:1 and 5:1. The resulting structures were investigated using transmission electron microscopy (TEM), selected area electron diffraction (SAED), dynamic light scattering (DLS), wide-angle X-ray scattering (WAXS), and atomic force microscopy (AFM) techniques. Finally, possible mechanisms that account for the formation of the observed micellar morphologies are discussed.

RESULTS

Synthesis and Characterization of PFS-*b*-P2VP Diblock Copolymers. Two samples of PFS-*b*-P2VP diblock copolymers with different block ratios, PFS_{74}-*b*-$P2VP_{74}$ (1:1) and PFS_{120}-*b*-$P2VP_{24}$ (5:1), were synthesized via sequential living anionic polymerization using a previously described method (Scheme 1).[7,25] First, the polymerization of dimethylsila[1]ferrocenophane (**1**) was performed in THF at room temperature using *n*-BuLi as an initiator. An aliquot of the reaction mixture was taken for molecular weight analysis using gel permeation chromatography (GPC), before 1,1-dimethylsilacyclobutane (DMSB) and 1,1-diphenylethylene (DPE) were added. DMSB serves as a carbanion pump[26,27] that facilitates the coupling of living PFS to DPE. DPE acts as an end-capping agent to avoid side reactions upon the addition of 2-vinylpyridine. Rehahn et al. reported that 1−3 units of silacyclobutane are required for the efficient anionic chain end transfer to DPE.[25] The polymerization of 2-vinylpyridine was allowed to proceed for 2 h at −78 °C before the reaction mixture was quenched by adding a few drops of degassed

Scheme 1. Synthesis of PFS-*b*-P2VP Diblock Copolymers via Sequential Living Anionic Polymerization

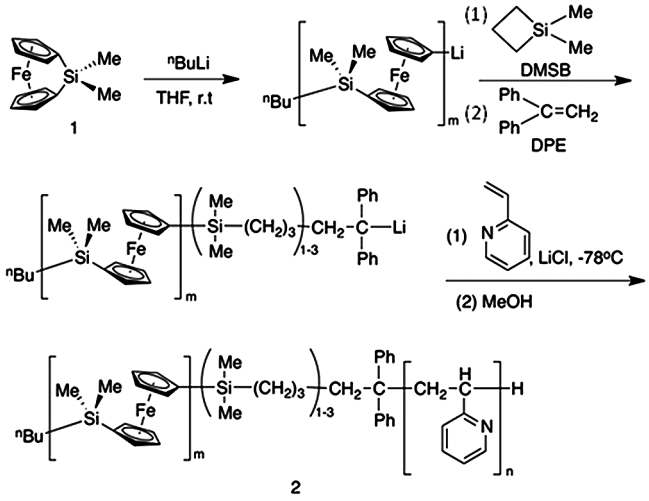

PFS_m-*b*-$P2VP_n$ m:n = 1:1, 5:1

methanol. PFS-*b*-P2VP diblock copolymers were precipitated into rapidly stirring hexane, and the polydispersities (PDIs) of the resulting materials were determined using GPC (see Figure S1). The block ratio and molecular weight of the block copolymers was obtained from ^{1}H NMR spectra via the integration of characteristic signals from both blocks (Figures S2 and S3), and a comparison to the absolute molecular weight of the homopolymers was determined by GPC. The characterization data for the block copolymers studied here are reported in Table 1.

Table 1. Characterization Data for the PFS-*b*-P2VP Diblock Copolymers

PFS_m-*b*-$P2VP_n$	M_n^{PFS} (g/mol)[a]	$M_n^{PFS\text{-}b\text{-}P2VP}$ (g/mol)[b]	theor $M_n^{PFS\text{-}b\text{-}P2VP}$	N^{PFS}/N^{P2VP}[b]	PDI[a]
PFS_{74}-*b*-$P2VP_{74}$	17 900	25 700	24 300	1:1	1.12
PFS_{120}-*b*-$P2VP_{24}$	29 000	31 700	27 400	5:1	1.09

[a]Determined by GPC analysis. [b]Calculated from the relative ^{1}H NMR integration. Subscripts represent number-averaged degrees of polymerization.

Self-Assembly Studies of PFS-*b*-P2VP Diblock Copolymers. The procedures for achieving the self-assembly of the PFS-*b*-P2VP samples with different block ratios (1:1 and 5:1) in dilute solution are described as follows utilizing PFS_{74}-*b*-$P2VP_{74}$ as an example. Three different methods were used. In the first method, a micelle solution of PFS_{74}-*b*-$P2VP_{74}$ was prepared by first dissolving the sample in THF. To induce self-assembly of PFS_{74}-*b*-$P2VP_{74}$, *i*PrOH, a selective solvent for the P2VP block, was added very slowly (∼1 drop every 5 s) to a clear solution of PFS_{74}-*b*-$P2VP_{74}$ in THF. A range of different solvent ratios was chosen for the self-assembly via this method, namely THF/*i*PrOH, 10/90, 20/80, 30/70, and 40/60 vol %.

To explore the effect of the sequence of solvent addition on the final micelle morphology, a second (inverse self-assembly) and a third (direct mixing) preparative methods were also used. The inverse self-assembly was performed by first suspending the PFS_{74}-*b*-$P2VP_{74}$ in *i*PrOH, followed by the slow addition of

dx.doi.org/10.1021/ma2027726 | Macromolecules 2012, 45, 3883−3891

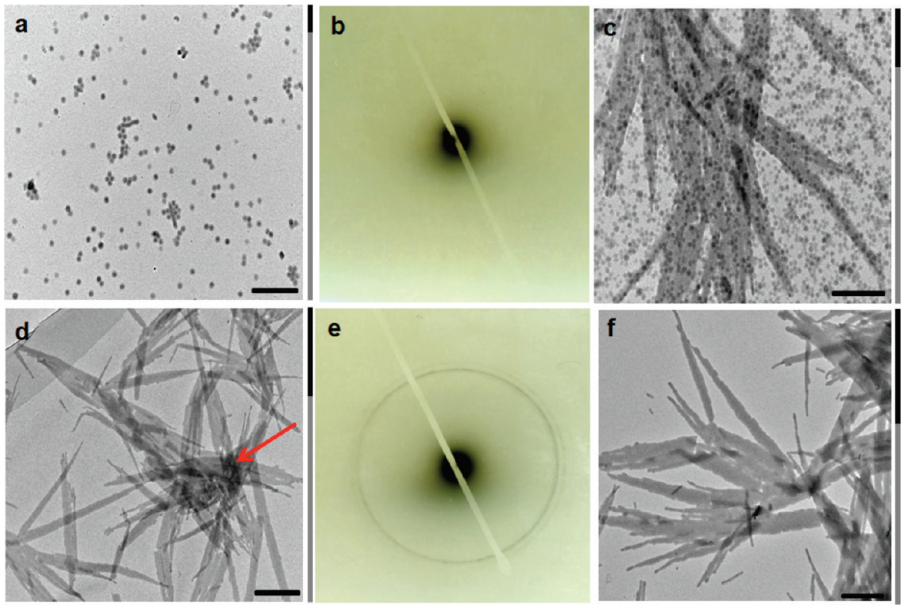

Figure 1. TEM images and SAED patterns of micelle morphologies for PFS_{74}-*b*-$P2VP_{74}$ in different THF/*i*PrOH mixtures after aging for 18 h at room temperature: (a) spherical micelles in 10/90 (v/v), (b) SAED pattern of spherical micelles in (a), (c) coexisting platelets and spherical micelles in 20/80 (v/v), (d) platelets in 30/70 (v/v), (e) SAED pattern of platelet micelles in (d), (f) TEM image of platelet micelles in 40/60 (v/v). Black and gray lines represent the percentage of THF and *i*PrOH present in the solution, respectively. Scale bars correspond to 500 nm.

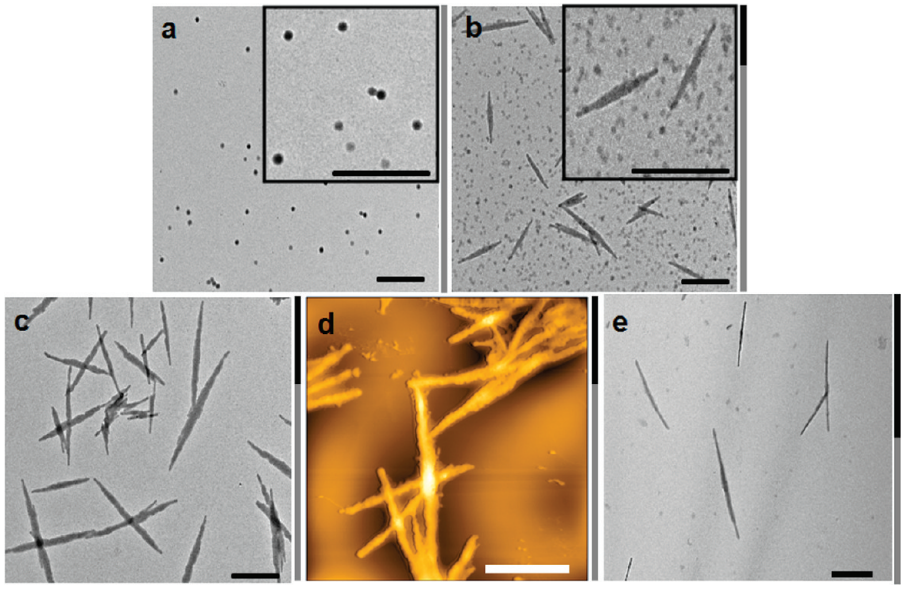

Figure 2. TEM images obtained by increasing the quantity of added THF into PFS_{74}-*b*-$P2VP_{74}$/*i*PrOH suspensions: (a) spherical micelles (100% *i*PrOH), (b) coexisting spheres and lenticular-shaped platelets (THF/*i*PrOH; 20/80, v/v %), (c) lenticular-shaped platelet micelles (THF/*i*PrOH; 30/70, v/v %), (d) tapping mode AFM height image of lenticular-shaped platelet micelles shown in (c), (e) lenticular-shaped platelet micelles (THF/*i*PrOH; 50/50, v/v %). Black and gray lines represent the percentage of THF and *i*PrOH present in the solution, respectively. Insets in (a) and (b) represent higher magnification images. Scale bars correspond to 500 nm.

the common solvent THF to achieve the same solvent ratio as the first method. The solution was then heated to 70 °C for 1 h and subsequently cooled to room temperature at a cooling rate of 0.5 °C/min. The direct mixing method was implemented as follows. PFS_{74}-*b*-$P2VP_{74}$ diblock copolymer was dissolved in a THF/*i*PrOH solvent mixture at 70 °C for 1 h, and the solution was then cooled to room temperature at the rate of 0.5 °C/min. All micelle solutions from three different methods were kept at a concentration of 0.5 mg/mL (~0.05 wt %) and were aged for 18 h at room temperature prior to TEM imaging.

Self-Assembly of PFS_{74}-b-$P2VP_{74}$ (1:1). The solution self-assembly of PFS_{74}-*b*-$P2VP_{74}$ (1:1) was studied using the first method by dissolution of PFS_{74}-*b*-$P2VP_{74}$ in THF followed by the dropwise addition of *i*PrOH. The micelle solutions were prepared in four different ratios of THF/*i*PrOH; 10/90, 20/80, 30/70, and 40/60 vol %. Figure 1 shows a set of bright field TEM micrographs and the corresponding selected area electron diffraction (SAED) patterns of the resulting PFS_{74}-*b*-$P2VP_{74}$ micelles after 18 h followed by solvent evaporation. At low THF content (THF/*i*PrOH = 10/90 v/v), we observed exclusively spherical micelles of ~10 nm diameter by TEM

dx.doi.org/10.1021/ma2027726 | *Macromolecules* 2012, 45, 3883–3891

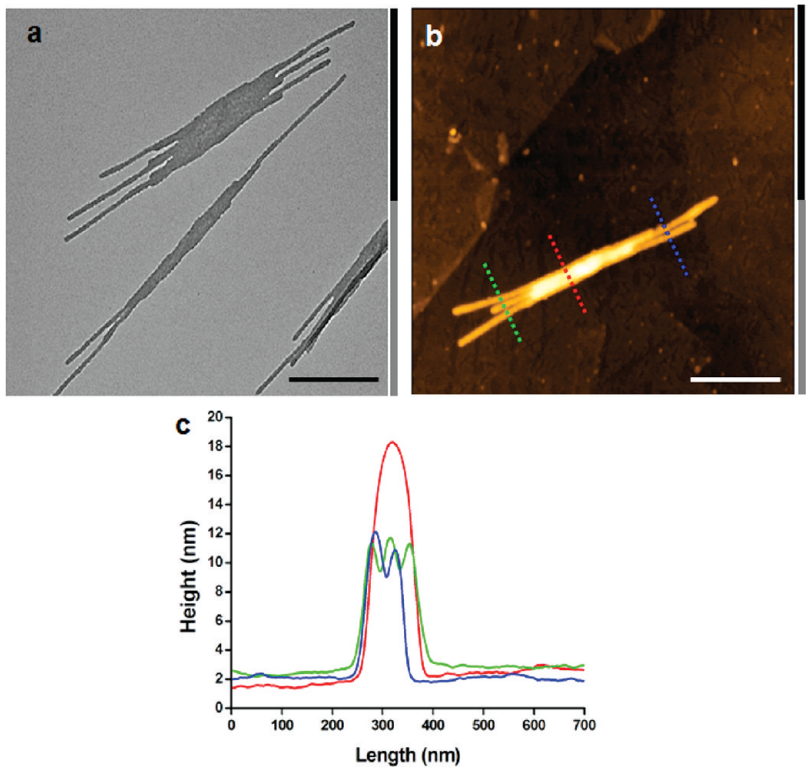

Figure 3. (a) TEM image; (b) tapping mode AFM height image of aggregated lenticular platelet micelles of PFS_{74}-*b*-$P2VP_{74}$ obtained in a mixture of THF/*i*PrOH (50/50, v/v %) via the second method after aging the solution for 3 days at room temperature; (c) AFM height profiles of aggregated lenticular platelet micelles collected in three different regions. Black and gray lines represent the percentage of THF and *i*PrOH present in the solution, respectively. Scale bars correspond to 500 nm.

(Figure 1a). The spheres represent only the organometallic core-forming block because of the high electron density of the PFS domains. In addition, prior to TEM analysis, the diameter of the spherical micelles in dilute solution was measured by DLS. The value, which includes the contribution from the corona, was ~15 nm (Figure S4). The SAED pattern of the spherical micelles shown in Figure 1b displayed only diffuse amorphous rings and indicated that the PFS core is amorphous.

At a THF concentration of 20 vol % (20/80 v/v), TEM showed the coexistence of platelets and spherical micelles (Figure 1c). When the THF concentration was further increased to 30 vol % (30/70 v/v), exclusively platelet micelles (Figure 1d) were detected. The corresponding SAED pattern is also shown in Figure 1e, and the presence of well-defined diffraction rings indicated that the PFS core is crystalline. The platelet micelles comprised isolated structures and aggregates. It is noteworthy that platelet aggregates indicated by the red arrow are formed by the sequential stacking of a series of platelets together. The rough-edged crystalline platelet micelle morphology still remained as shown in Figure 1f when the THF concentration was further increased to 40 vol %.

To explore whether the sequence of solvent addition affected the final micelle morphology, solutions of PFS_{74}-*b*-$P2VP_{74}$ (0.5 mg/mL) in THF/*i*PrOH having different volume ratios (20/80, 30/70, and 50/50 vol %) were prepared by the inverse self-assembly procedure (the second method). Figure 2 shows a set of TEM images of the micelle morphology evolution on increasing the THF content of the PFS_{74}-*b*-$P2VP_{74}$/*i*PrOH suspension. In pure *i*PrOH, the block copolymer formed a suspension due to the poor solubility of the material in this solvent. However, a pale yellow solution was observed due to partially dissolved PFS_{74}-*b*-$P2VP_{74}$ block copolymer after heating at 70 °C for 1 h. Spherical micelles were observed after dropping a solution of PFS_{74}-*b*-$P2VP_{74}$ micelles in *i*PrOH onto TEM grids (Figure 2a). After slow addition of THF into *i*PrOH and heating the resulting mixture to 70 °C for 1 h, a coexistence of both spherical and platelet-shaped-like micelles was detected by TEM at a THF/*i*PrOH 20/80 (v/v) (Figure 2b). Furthermore, the platelet micelles in Figure 2b exhibited a "lenticular" shape with a high aspect ratio and with rough and curved edges.

Similar lenticular platelets were exclusively observed by TEM for solvent ratios of THF/*i*PrOH 30/70 (v/v) and 50/50 (v/v) as shown in Figure 2c–e.[28] These structures were further characterized by AFM as shown in Figure 2d. A height profile showed that the thickness of this lenticular lamellar structure was ~20 nm. This result is consistent with a lenticular-shaped platelet micelle having a thin layered sandwich structure consisting of chain-folded PFS lamellar crystals covered by two glassy P2VP layers (T_g^{P2VP} = 104 °C).[29] Interestingly, when the micelle solution with a THF/*i*PrOH 50/50 (v/v) ratio was further kept at room temperature for 3 days, aggregated, irregular structures with a multilenticular form were generated (Figure 3). We speculate that these aggregates arise where two or three platelet nuclei are formed during the nucleation step and then subsequently grow into the observed nanostructures over time.

As noted above, a third self-assembly method (direct mixing) was also employed for PFS_{74}-*b*-$P2VP_{74}$ in THF/*i*PrOH. A similar micelle morphology evolution associated with increasing THF content was observed, and the corresponding TEM and AFM results are shown in Figure S5a–f. It was possible to

dx.doi.org/10.1021/ma2027726 | *Macromolecules* 2012, 45, 3883–3891

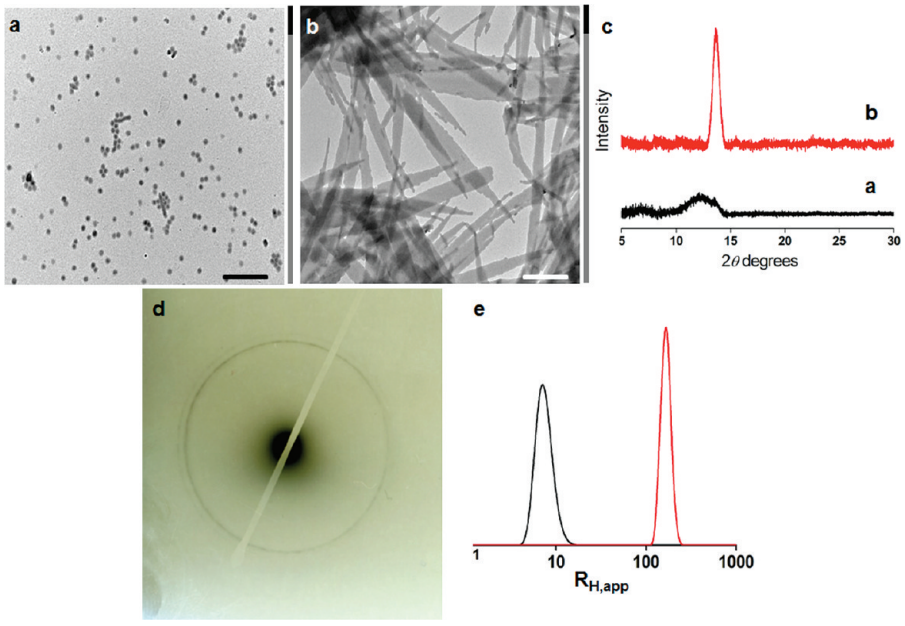

Figure 4. TEM images of PFS_{74}-*b*-$P2VP_{74}$ micelles prepared in THF/*i*PrOH (10/90 v/v %) after (a) 1 day and (b) 30 days, (c) WAXS profiles of the PFS_{74}-*b*-$P2VP_{74}$ micelles for (a) spheres and (b) platelets. The WAXS samples were prepared by casting a 3 day old solution of micelles onto a silicon wafer and allowing the solvent to evaporate at ambient temperature, (d) SAED pattern of aggregated lenticular platelets, (e) DLS measurements of micelles in 10/90 (v/v %): black curve (after 1 day), red curve (after 30 days). Note: a morphological transformation was also observed in the 20/80 (v/v %) case from a coexistence of spherical micelles and platelets (Figures 1c, 2b, and S7a and S8a) to exclusively platelet micelles (Figure S7 and S8) after aging for 6 months at room temperature. Black and gray lines represent the percentage of THF and *i*PrOH present in the solution, respectively. Scale bars correspond to 500 nm.

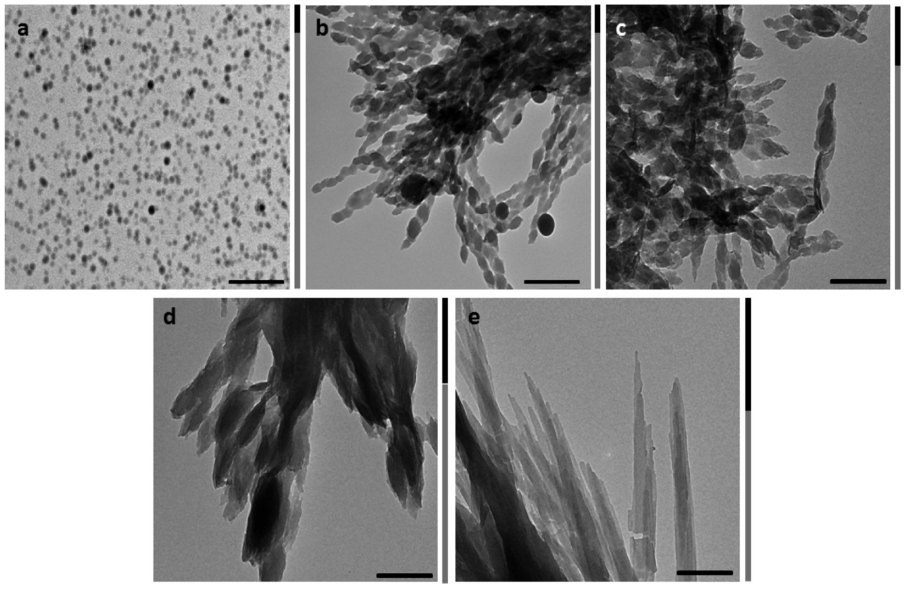

Figure 5. TEM images of micelles formed by PFS_{120}-*b*-$P2VP_{24}$ in THF/*i*PrOH prepared via the first protocol: (a) spherical micelles in THF/*i*PrOH (10/90, v/v) after 1 day, (b) irregular ill-shaped platelets in 10/90 (v/v) after 30 days, (c) large lenticular-shaped platelets aggregates observed in 40/60 (v/v) after 30 days, (d) irregular ill-shaped platelets in 20/80 (v/v), and (e) large lenticular platelets in 30/70 (v/v). Note: for all solvent ratios, spherical micelles were formed after 1 day and self-assembly into crystalline platelets occurred within 30 days (b–e). Black and gray lines represent the percentage of THF and *i*PrOH present in the solution, respectively. Scale bars correspond to 500 nm.

collect the height profile of an isolated crystalline lenticular PFS_{74}-*b*-$P2VP_{74}$ micelle by AFM. The height profiles of the center and edges of two lenticular micelles in Figure S5d show that the thickness of the center (~14–16 nm) is larger than that of the edges (~8 nm). The thick center portion of the platelet is attributed to the nuclei of the PFS lamellar crystals,[34,37] and a similar crystal morphology was observed previously in the case of lamellar single crystals of poly(styrene-*b*-ethylene oxide) grown in dilute solution.[17] Again, when the micelle solution formed in THF/*i*PrOH 50/50 (v/v) was kept at room temperature for a further 3 days, aggregated crystalline lenticular platelet micelles were formed (Figure S6). The dominant lenticular-shaped platelets shown in Figures 1, 2, and S5 were found to be stable over several months, suggesting that

dx.doi.org/10.1021/ma2027726 | *Macromolecules* 2012, 45, 3883–3891

lenticular lamellar nanostructures represent the equilibrium state.

Time-Dependent Morphological Transitions for PFS_{74}-b-P2VP$_{74}$ (1:1). To confirm whether the spherical micelles formed using the first method (Figure 1a) represent a metastable or kinetically "quenched" morphology which evolves to the thermodynamically preferred morphology over time, we repeated TEM analysis after keeping the micelles at room temperature for 1 month. For the spherical micelles formed in THF/*i*PrOH (10/90, v/v %) via the first method, a morphological transition from spheres to lenticular platelets was observed by TEM (see Figure 4a,b).

The 1D WAXS (Figure 4c) showed a strong diffraction peak with d = 6.4 Å (2θ = 13.53°) and SAED (Figure 4d) profile of the PFS platelet aggregates in Figure 4b confirmed the crystalline nature of the lenticular platelets.[7] DLS results were also qualitatively consistent with the assigned change in micelle morphology and showed a substantial increase in the micelle size after 30 days (Figure 4e).[30] In addition, this morphological transition was also detected in THF/*i*PrOH solvent mixtures with different compositions. For example, coexisting spheres and platelets were initially observed in THF/*i*PrOH 20/80 (v/v) for all three different preparation protocols as shown in Figures 1c, 2b, and S5a. These mixed micellar morphologies were found to transform into lenticular platelets exclusively (see Figures S7, S8, and S9). We therefore consider the lenticular structures as an equilibrium morphology, whereas the spherical micelles are probably kinetically trapped.[31,34b]

Self-Assembly of PFS_{120}-b-P2VP$_{24}$ (5:1). The influence of the block ratio on the solution self-assembly of PFS-*b*-P2VP samples was addressed utilizing the PFS_{120}-*b*-$P2VP_{24}$ diblock copolymer. In the case of PFS_{120}-*b*-$P2VP_{24}$, the block length ratio is more asymmetric (5:1) and the crystallizable PFS segment comprises the major block. Therefore, the crystallization of the PFS majority block expected to dominate the resulting micelle morphology. Micellar solutions from PFS_{120}-*b*-$P2VP_{24}$ were prepared utilizing method 1. Initially, spherical micelles were obtained for all solvent ratios (THF/*i*PrOH; 10/90, 20/80, 30/70, and 40/60 v/v) after aging for 1 day at room temperature (Figure 5a). TEM results confirmed that the morphological transition of the micelles from spheres into irregular ill-shaped platelets (Figure 5b, THF/*i*PrOH 10/90 v/v), and the formation of lenticular platelets occurred within 1 month (Figure 5c, 40/60 v/v). Under conditions of similar solvent blending ratio, where the volume fraction of THF was greater than 10%, PFS_{120}-*b*-$P2VP_{24}$ required a significantly longer time to form lenticular-shaped platelets (1 month compared to 18 h). In addition, a higher tendency for aggregation of the platelets was found if compared to PFS_{74}-*b*-$P2VP_{74}$.

DISCUSSION

The spherical micelles formed by PFS_{74}-*b*-$P2VP_{74}$ (1:1) shown in Figure 1a presumably consist of a PFS core, surrounded by a coronal layer of P2VP. We consider this to be a kinetically trapped morphology due to an amorphous PFS core, as demonstrated by the diffuse amorphous ring observed from the SAED (Figure 1b). In contrast, the diffraction pattern (Figure 1e) obtained for PFS-*b*-P2VP platelets shows that the cores of these structures are crystalline. Significantly, the SAED pattern showed two isotropic diffraction rings. Based on the X-ray diffraction patterns of PFS homopolymer films reported by Papkov and co-workers, the strong inner ring with a d-spacing of 0.60 nm was indexed as a (010) plane while the weak outer ring was assigned to overlapping ($1\bar{1}0$) and (110) diffraction planes with a d-spacing of 0.56 nm based on PFS crystallography.[32] On the other hand, similar staggered crystalline platelets have been reported for both homopolymer and diblock copolymer single crystals grown in dilute solution or the crystallization of crystalline-coil diblock copolymers in thin films.[33,34a] The spiral overgrowths of the PFS crystals can be achieved by the growth in one crystalline platelet micelle initiating that of another adjacent platelet micelle through a screw dislocation effect.[34]

In contrast to the elongated ribbon-shaped single-crystal-like PI_{76}-*b*-PFS_{76} micelles formed in xylene/decane (1:10 v/v)[21a] that exhibited three pairs of strong diffraction spots in the SAED pattern,[19b] the pattern for the lenticular-shaped PFS-*b*-P2VP platelet aggregates only suggests that they are crystalline structures. Comparison of the platelet micelles obtained from the third method to those formed by the first and second methods indicated that the lenticular-shaped micelle morphology in Figure S5 showed a lower degree of aggregation even at similar concentrations of 0.5 mg/mL. This indicated that the preparation procedures do not affect the overall micelle morphology but do influence the difference in the degree of aggregation of the lenticular micelles at the same solution concentration. In addition, as noted above, the PFS_{74}-*b*-$P2VP_{74}$ micelles in THF/*i*PrOH 50/50 prepared using method 2 and 3 were shown to form less aggregated crystalline lenticular micelles after aging for several days at room temperature. It can be assumed that the presence of a large amount of THF leads to a plastization of the PFS core. This then increases the overall solubility of PFS-*b*-P2VP diblock copolymers and might lead to a higher colloidal stability and, hence, a lower tendency for aggregation of the platelets.

The difference in both the growth rate of platelets and the degree of platelet aggregation between the 1:1 block copolymer PFS_{74}-*b*-$P2VP_{74}$ and the analogous 5:1 material PFS_{120}-*b*-$P2VP_{24}$ is probably attributed to the crystallization characteristics of the metal-containing PFS core-forming block. It has been reported that PFS homopolymers possess a rather slow crystal growth rate and a low degree of crystallinity in the bulk state.[35] The existence of rigid, bulky ferrocene groups in the PFS main chain might contribute to the apparent difficulty in the chain packing process involved with the formation of PFS crystals.[32,36] In addition, a decrease in the degree of the crystallinity with increasing molecular weight was found by DSC analysis as published by Vancso and co-workers.[36] Our results indicate that the molecular weight of the PFS block also influences the growth rate of the crystalline PFS-*b*-P2VP micelles in solution, visible through different growth times necessary for the transformation of spherical structures into lenticular platelets.[37] Thus, a longer time (30 days) was needed for PFS_{120}-*b*-$P2VP_{24}$ (5:1), if compared to PFS_{74}-*b*-$P2VP_{74}$ (1:1) (18 h) for the PFS chains to crystallize and form platelet micelles (see Figures 1 and 5).

Crystallization-driven morphological sphere-to-rod or sphere-to-platelet transitions have been recently reported for micelles derived from several different crystalline-coil diblock copolymer systems such as asymmetric PFS-*b*-P2VP,[7,14] PCL-*b*-PEG (polycaprolactone-*b*-poly(ethylene glycol)),[15] and PB-*b*-PEO (polybutadiene-*b*-poly(ethylene oxide)).[38−40] Thereby, the changes in micellar morphology were achieved by controlling the solution environment and/or the crystallization temperature,[16,38−40] the amount of an inorganic salt present,[41]

dx.doi.org/10.1021/ma2027726 | Macromolecules 2012, 45, 3883−3891

the micelle concentration,[15] and the temperature-dependent solvent quality.[16] In general, the morphologies observed for crystalline micelles with different interfacial curvature (spheres, cylinders, or platelets) are governed by the competition between (1) the crystallization of the crystalline core-forming block, which favors the growth of the platelets, and (2) the stretching of the corona-forming block, which favors curvature of the core−corona interface and confines the lateral platelet growth. Indeed, the solvent conditions would be expected to influence the relative strength of these two competing factors. In this study it is suggested that the change in solvent quality forces the morphological transition from amorphous spherical micelles to crystalline PFS-*b*-P2VP platelet micelles by mixing THF and *i*PrOH. It is likely that an increasing amount of THF, a good solvent for PFS, allows the solvent to function as a "plasticizer" for the PFS core, thereby facilitating crystallization.

In principle, crystalline polymers with a low rotational symmetry unit cell possess anisotropic single crystal habits such as ribbons.[34] The observation of elongated ribbon-shaped or tape-like PFS platelets in solution[19b,21a] or melt crystallization[42] experiments is consistent with this principle due to the fact that the PFS monoclinic unit cell possesses low helical 2^1 rotational symmetry.[32,34] Initially, free chains in solution undergo homogeneous nucleation to form a number of nuclei that serve as the templates for the crystal growth. Consequently, other free chains containing the PFS block will then deposit on the crystal growth fronts or the edges of the platelet, accompanied by secondary nucleation and growth steps (epitaxial crystallization) leading to further growth of the platelet.

To explain the formation of the rough, round lenticular-shaped crystalline PFS-*b*-P2VP platelets (Figure 6), we

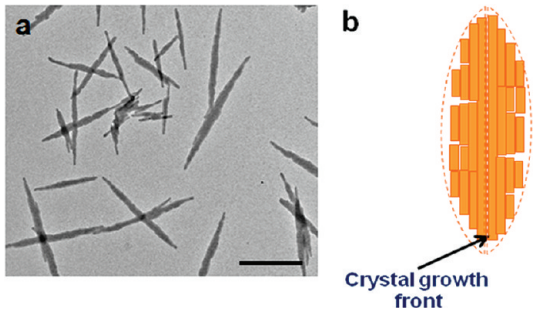

Figure 6. (a) Lenticular-shaped micelles, (b) a hypothesized growth mechanism for the formation of the lenticular platelet micelles with PFS crystalline core (top view) for PFS_{74}-*b*-$P2VP_{74}$ in THF/*i*PrOH (30/70, v/v), and two covered glassy P2VP layers are not illustrated here. The scale bar corresponds to 500 nm.

speculate that the P2VP corona-forming blocks have a significant interference effect on the crystal growth fronts during the crystal growth process. In contrast to the formation of smooth ribbon-like PFS single crystals from the melt,[42] the observation of lenticular PFS-*b*-P2VP platelets in solution suggests that the crystal growth fronts of the crystalline PFS-*b*-P2VP platelets are likely to be "poisoned" by the P2VP corona-forming blocks during the growth step in THF/*i*PrOH solvent mixtures.[43] The poisoning effect might originate from defects on the crystal growth front created by the interference of the P2VP corona blocks with the PFS crystal growth. These defects would then affect the deposition of PFS blocks at the crystal growth fronts leading to the rough (defect-containing) surfaces which would result in the formation of lenticular-shaped micelles (Figure 6b). Furthermore, this poisoning effect might also change the rates of secondary nucleation and the radial growth occurring on the PFS crystal growth fronts. Significantly, the influence of poisoning effects on the platelet morphology is further supported by solution self-assembly of two other crystalline PFS-*b*-coil diblock copolymers having amorphous corona blocks under different conditions. These include the crystalline pointed oval shaped PFS-*b*-PP (PP = polyphosphazene) micelles formed by adding PFS-*b*-PP to the PFS-*b*-P2VP seed micelles in isopropanol[44] and the lenticular-shaped PS-*b*-PFS (PS = polystyrene) platelets formed in dichloromethane when the crystallization of the core PFS blocks took place at a low degree of oxidation (x = 0.25).[45] Interestingly, preliminary studies regarding the solution self-assembly of both PI-*b*-PFS (PI = polyisoprene)[19b,21a] and PFS-*b*-PDMS (PDMS = polydimethylsiloxane)[46] samples with short corona-forming blocks led to platelet micelles possessing regular surfaces. This suggested that poisoning effects might be less significant for a PFS-*b*-coil diblock copolymer having a short flexible corona-forming block under the conditions investigated. Further work in this area is in progress and our results will be reported in the near future.

■ SUMMARY

Two well-defined crystalline-coil PFS-*b*-P2VP diblock copolymers with different block ratios (1:1 and 5:1) were synthesized via sequential living anionic polymerization. The effect of solvent quality on the micellar morphologies formed by these two PFS-*b*-P2VP samples was addressed by a combination of TEM, SAED, DLS, WAXS, and AFM techniques. Results showed that for PFS-*b*-P2VP (block ratios 5:1 or 1:1) the resulting micelles undergo a sphere-to-platelet transition over time in THF/*i*PrOH solvent mixtures with less than 30 vol % THF. Both SAED and WAXS data supported the assertion that in mixed solvents the PFS-*b*-P2VP platelet micelle formation is driven by the crystallization of the PFS core. Furthermore, the molecular weight of the crystallizable PFS block was found to affect the rate of the sphere-to-platelet transition. Thus, a substantially longer time was needed for the longer PFS block present in PFS_{120}-*b*-$P2VP_{24}$ (5:1) to crystallize and a sphere-to-platelet transition to take place. Lenticular-shaped PFS-*b*-P2VP platelets were observed as the dominant morphology irrespective of the block ratio as the concentration of THF increased at or beyond 30 vol %. The formation of lenticular rather than regular platelets was attributed to a poisoning effect whereby interference of the P2VP corona-forming blocks in the growth of the crystalline PFS core leads to the creation of defects in the crystal growth fronts.

■ EXPERIMENTAL PART

General Methods. Dimethylsila[1]ferrocenophane was synthesized according to a previous methodology reported in the literature.[47] All chemicals were used as received from Aldrich unless stated otherwise. *n*-Butyllithium (1.6 M in hexanes, Acros) and trioctylaluminum (25 wt % in hexanes) were used as received. 2-Vinylpyridine was purified by distillation first over CaH_2. A second distillation from trioctylaluminum was performed immediately before polymerization. 1,1-Diphenylethylene (DPE) was distilled once over CaH_2. 1,1-Dimethylsilacyclobutane (DMSB) (Fluka) was distilled over CaH_2 twice. Lithium chloride was vacuum-dried at 120 °C overnight. Prior to use, tetrahydrofuran was distilled from Na/benzophenone under reduced pressure. Methanol, used for quenching the polymers, was deoxygenated by bubbling with N_2. All polymerizations were

conducted in a MBraun MB 150-BG inert atmosphere glovebox purged with purified argon. All reagents distillations and monomer synthesis were carried out using Schlenk line techniques in a ventilated fume hood. ^{1}H NMR was performed on Jeol CX270 and GX400 at 270 and 400 MHz, respectively.

Gel permeation chromatographies (GPC) for homopolymers were performed using a Viscotek VE 2001 triple detection gel permeation chromatograph, equipped with an automatic sampler, a pump, an injector, an inline degasser, a column oven (30 °C), and RI, viscometry, and light scattering detectors. THF was used as the eluent with a flow rate 1.0 mL/min. Samples were dissolved in THF (2 mg/mL) before analysis. Meanwhile, diblock copolymers were characterized using GPC in THF with 0.1% *n*-Bu_4NBr solution to provide PDI data, and the block ratios were obtained from integrated ^{1}H NMR signals from each block. The molecular weight of the block copolymer was then calculated from that of the homopolymer as determined by triple detection GPC studies. Block copolymer samples were dried in a Shell Laboratory vacuum oven, equipped with a nitrogen purge line.

Copper grids from Agar Scientific, mesh 400, were coated with a carbon film. Carbon coating was performed using Agar TEM Turbo Carbon Coater, where carbon was sputtered onto mica sheets before deposition on the grids via floatation.

TEM samples for electron microscopy were prepared by drop-casting one drop (ca. 10 μL) of the micelle solution onto carbon-coated copper grid placed on a piece of filter paper to remove excess solvent. Because of the high iron content of the PFS block, it was not necessary to stain the samples to obtain higher contrast. Transmission electron microscopy (TEM) was performed on both Jeol 1200EX TEM Mk1 and Mk2 which operates with a tungsten filament at 120 kV. They are fitted with MegaViewII digital cameras, with the Soft Imaging Systems FmbH analysis with image analysis software (3.0 versions). Electron diffraction (ED) was carried out using Jeol 1200EX Mk1. The *d*-spacings of SAED patterns were calibrated using a TlCl standard.

Atomic force microscopy (AFM) studies were conducted in tapping mode using a multimode atomic force microscope equipped with a Nanoscope III controller (Veeco Instruments Ltd., Santa Barbara, CA). PPP NHCR10 long cantilever-type probes with ca. 10 nm tip radii were employed. The samples were prepared by drop-casting solutions of micelles (ca. 0.05 mg/mL) onto freshly cleaved highly ordered pyrolytic graphite (HOPG). Imaging was conducted in air at ambient temperature. Images were analyzed using Gwyddion, an open source software program for SPM images.

Wide-angle X-ray diffraction (WAXS) data were recorded using a Bruker-AXS D8 Advance diffractometer. The wavelength of the X-ray beam was 0.154 18 nm. 1D WAXD profiles were calibrated using α-Al_2O_3 with known crystal diffraction at $2\theta = 28.47°$.

Dynamic light scattering (DLS) was carried out using Malvern Zetasizer Nano Series equipped with a laser with a wavelength of 633 nm and a detector oriented at 173° to the incident radiation.

Synthesis of PFS-*b*-P2VP Block Copolymers. The synthesis of 1:1 block copolymer PFS_{74}-*b*-$P2VP_{74}$ is described and is representative. In a N_2-filled glovebox at room temperature, 12.0 μL of *n*-BuLi (1.6 M in hexanes) was added quickly to a stirred solution of dimethylsila[1]ferrocenophane (300 mg, 1.23 mmol) in THF (2.0 mL). After 40 min, the color of the solution changed from red to amber, indicating complete conversion of the monomer. DPE (14.0 μL, 0.08 mmol) was then added, followed by DMSB (3.0 μL, 0.04 mmol). This caused a change in color from amber to red within a minute. Living PFS solution and second flask containing a mixture of dried LiCl and 2-vinylpyridine (0.12 mL, 1.09 mmol) in 2 mL of THF were cooled to −78 °C before the two solutions were combined. The reaction was allowed to further proceed for 40 min at −78 °C before it was quenched by the addition of a few drops of degassed MeOH. Precipitation of the solution into hexanes followed by drying overnight under vacuum produced the product as a yellow powder (350 mg, 88%). The block copolymer PFS_{74}-*b*-$P2VP_{74}$ was purified by solvent partition using THF as a good solvent for both blocks and subsequent reprecipitation into hexanes. ^{1}H NMR δ (ppm, C_6D_6): 0.56 (s, $Si(CH_3)_2$), 1.84−2.93 (m, CH_2 and CH, P2VP), 4.12 (m, Cp), 4.28 (m, Cp), 6.33−7.10 (m, arH, P2VP), 8.40 (m, NCH-P2VP). GPC: M_n (PDI): 17 900 g/mol (1.04) for the PFS block and 25 700 g/mol (1.12) for the PFS_{74}-*b*-$P2VP_{74}$ diblock copolymer.

Solution Self-Assembly of PFS-*b*-P2VP. Three methods have been used to study self-assembly of two PFS-*b*-P2VP diblock copolymers in solution. Different solvent ratios were chosen for the self-assembly.

First method: the solvent blending ratio of THF to *i*PrOH was 10/90, 20/80, 30/70, and 40/60 vol %. In the first method, the micelle solution of PFS-*b*-P2VP was carried out by first dissolving sample in THF followed by the addition of *i*PrOH, very slowly (∼1 drop every 5 s). The micelle solutions were left to age for 18 h before TEM measurement.

The second method (inverse self-assembly) was performed by first suspending the PFS-*b*-P2VP in *i*PrOH followed by the addition of common solvent THF to achieve the specific solvent ratios. Later, the solutions were heated to 70 °C for 1 h, and these solutions were cooled to room temperature for 18 h prior to TEM imaging.

A third method (direct mixing) was performed as follows. PFS-*b*-P2VP diblock copolymer was dissolved in a mixed solvent of THF/*i*PrOH, and it was kept at 70 °C for 1 h; these solutions were cooled to room temperature, and the micelle solutions were left for 18 h prior to TEM imaging. All PFS-*b*-P2VP micelle solutions were kept at a concentration of 0.5 mg/mL (∼0.05 wt %).

■ ASSOCIATED CONTENT

Ⓢ Supporting Information

Full experimental details and characterization including additional GPC, ^{1}H NMR, DLS, TEM, and AFM data. This material is available free of charge via the Internet at http://pubs.acs.org.

■ AUTHOR INFORMATION

Corresponding Author

*E-mail: ian.manners@bristol.ac.uk (I.M.); mwinnik@chem.utoronto.ca (M.A.W.).

Present Address

⊥Institute of Organic and Macromolecular Chemistry and Jena Center for Soft Matter (JCSM), Friedrich-Schiller-University Jena, Lessingstraße 8, D-07743 Jena, Germany.

Notes

The authors declare no competing financial interest.

■ ACKNOWLEDGMENTS

S.F.M.Y. is grateful to the Ministry of Higher Education of Malaysia and Universiti Kebangsaan Malaysia for the provision of a Ph.D scholarship. M.-S.H. (European Union, Marie Curie) and F.H.S. (DAAD) are grateful for postdoctoral fellowships. I.M. thanks the European Union for a Marie Curie Chair and the European Research Council for an Advanced Investigator Grant and the Royal Society for a Wolfson Research Merit Award. M.A.W. also thanks NSERC of Canada for financial support. We thank Dr. Paul Rupar and Dr. Emma Dunphy for helpful discussions.

■ REFERENCES

(1) Qian, J.; Zhang, M.; Manners, I.; Winnik, M. A. *Trends Biotechnol.* **2010**, *28*, 84.
(2) Ding, J.; Liu, G.; Yang, M. *Polymer* **1997**, *38*, 5497.
(3) Klok, H.-A.; Lecommandoux, S. *Adv. Mater.* **2001**, *13*, 1217.
(4) Cheng, J. Y.; Mayes, A. M.; Ross, C. A. *Nat. Mater.* **2004**, *3*, 823.
(5) Krausch, G.; Magerle, R. *Adv. Mater.* **2002**, *14*, 1579.
(6) Zhang, L.; Eisenberg, A. *Science* **1995**, *268*, 1728.

(7) Wang, H.; Winnik, M. A.; Manners, I. *Macromolecules* **2007**, *40*, 3784.
(8) Gilroy, J. B.; Rupar, P. A.; Whittell, G. R.; Chabanne, L.; Terrill, N. J.; Winnik, M. A.; Manners, I.; Richardson, R. M. *J. Am. Chem. Soc.* **2011**, *133*, 17056.
(9) Korczagin, I.; Hempenius, M. A.; Fokkink, R. G.; Cohen-Stuart, M. A.; Al-Hussein, M.; Bomans, P. H. H.; Frederik, P. M.; Vancso, G. J. *Macromolecules* **2006**, *39*, 2306.
(10) Bates, F. S. *Science* **1991**, *251*, 898.
(11) Discher, D. E.; Eisenberg, A. *Science* **2002**, *297*, 967.
(12) Cameron, N. S.; Corbiere, M. K.; Eisenberg, A. *Can. J. Chem.* **1999**, *77*, 1311.
(13) Yu, K.; Eisenberg, A. *Macromolecules* **1998**, *31*, 9399.
(14) (a) Shen, L.; Wang, H.; Guerin, G.; Wu, C.; Manners, I.; Winnik, M. A. *Macromolecules* **2008**, *41*, 4380. (b) He, F.; Gädt, T.; Manners, I.; Winnik, M. A. *J. Am. Chem. Soc.* **2011**, *133*, 9095. (c) Wang, H.; Lin, W.; Fritz, K. P.; Scholes, G. D.; Winnik, M. A.; Manners, I. *J. Am. Chem. Soc.* **2007**, *129*, 12924.
(15) Fairley, N.; Hoang, B.; Allen, C. *Biomacromolecules* **2008**, *9*, 2283.
(16) Mihut, A. M.; Drechsler, M.; Möller, M.; Ballauff, M. *Macromol. Rapid Commun.* **2010**, *31*, 449.
(17) (a) Lotz, B.; Kovacs, A. J. *Colloid Polym. Sci.* **1966**, *209*, 97. (b) Lotz, B.; Kovacs, A. J.; Bassett, G. A.; Keller, A. *Colloid Polym. Sci.* **1966**, *209*, 115. (c) Kovacs, A. J.; Lotz, B.; Keller, A. J. *Macromol. Sci. Phys.* **1969**, *B3* (3), 385.
(18) (a) Wang, X.; Liu, K.; Arsenault, A. C.; Rider, D. A.; Ozin, G. A.; Winnik, M. A.; Manners, I. *J. Am. Chem. Soc.* **2007**, *129*, 5630. (b) Wang, H.; Wang, X.; Winnik, M. A.; Manners, I. *J. Am. Chem. Soc.* **2008**, *130*, 12921. (c) Petzetakis, N.; Dove, A. P.; O'Reilly, R. K. *Chem. Sci.* **2011**, *2*, 955. (d) Du, Z.-X.; Xu, J.-T.; Fan, Z.-Q. *Macromolecules* **2007**, *40*, 7633. (e) Portinha, D.; Boué, L.; Bouteiller, L.; Carrot, G.; Chassenieux, C.; Pensec, S.; Reiter, G. *Macromolecules* **2007**, *40*, 4037. (f) Mihut, A. M.; Drechsler, M.; Möller, M.; Ballauff, M. *Macromol. Rapid Commun.* **2010**, *31*, 449. (g) Schmelz, J.; Karg, M.; Hellweg, T.; Schmalz, H. *ACS Nano* **2011**, *5*, 9523. (h) Lazzari, M.; Scalarone, D.; Vázquez-Vázquez, C.; López-Quintela, M. A. *Macromol. Rapid Commun.* **2008**, *29*, 352. (i) Patra, S. K.; Ahmed, R.; Whittell, G. R.; Lunn, D. J.; Dunphy, E. L.; Winnik, M. A.; Manners, I. *J. Am. Chem. Soc.* **2011**, *133*, 8842. (j) Gädt, T.; Schacher, F. H.; McGrath, N.; Winnik, M. A.; Manners, I. *Macromolecules* **2011**, *44*, 3777. (k) Gao, Y.; Li, X.; Hong, L.; Liu, G. *Macromoleculres* **2012**, *45*, 1321.
(19) (a) Wang, X.; Guerin, G.; Wang, H.; Wang, Y.; Manners, I.; Winnik, M. A. *Science* **2007**, *317*, 644. (b) Gädt, T.; Ieong, N. S.; Cambridge, G.; Winnik, M. A.; Manners, I. *Nat. Mater.* **2009**, *8*, 144. (c) Gilroy, J. B.; Gädt, T.; Whittell, G. R.; Chabanne, L.; Mitchels, J. M.; Richardson, R. M.; Winnik, M. A.; Manners, I. *Nat. Chem.* **2010**, *2*, 566.
(20) Lin, E. K.; Gast, A. P. *Macromolecules* **1996**, *29*, 390.
(21) (a) Cao, L.; Manners, I.; Winnik, M. A. *Macromolecules* **2002**, *35*, 8258. (b) Massey, J. A.; Temple, K.; Cao, L.; Rharbi, Y.; Raez, J.; Winnik, M. A.; Manners, I. *J. Am. Chem. Soc.* **2000**, *122*, 11577.
(22) Hsiao, M. S.; Chen, W. Y.; Zheng, J. X.; Van Horn, R. M.; Quirk, R. P.; Ivanov, D. A.; Thomas, E. L.; Lotz, B.; Cheng, S. Z. D. *Macromolecules* **2008**, *41*, 4794.
(23) Hsiao, M. S.; Zheng, J. X.; Leng, S. W.; Van Horn, R. M.; Quirk, R. P.; Thomas, E. L.; Chen, H. L.; Hsiao, B. S.; Rong, L. X.; Lotz, B.; Cheng, S. Z. D. *Macromolecules* **2008**, *41*, 8114.
(24) Hsiao, M. S.; Zheng, J. X.; Horn, R. M. V.; Quirk, R. P.; Thomas, E. L.; Chen, H. L.; Lotz, B.; Cheng, S. Z. D. *Macromolecules* **2009**, *42*, 8343.
(25) Kloninger, C.; Rehahn, M. *Macromolecules* **2004**, *37*, 1720.
(26) Sheikh, R. K.; Tharanikkarasu, K.; Imae, I.; Kawakami, Y. *Macromolecules* **2001**, *34*, 4384.
(27) Sheikh, R. K.; Imae, I.; Tharanikkarasu, K.; LeStrat, V. M. J.; Kawakami, Y. *Polym. J.* **2000**, *32*, 527.
(28) The collection of a SAED pattern for several lenticular crystalline platelets prepared using the second method (Figure 2c) was difficult to achieve due to the short lifetime of the diffraction.
(29) Brandrup, J.; Immergut, E. H.; Grulke, E. A.; Abe, A.; Bloch, D. R. *Polymer Handbook*; John Wiley & Sons: New York, 2003.
(30) In many cases, the sizes obtained from DLS measurements were not consistent with the cross sections of the platelets observed by TEM. This is presumably a consequence of the poor approximation of the platelet micelles to solid spheres employed by the Malvern Dispersion Technology Software (DTS).
(31) Hayward, R. C.; Pochan, D. J. *Macromolecules* **2010**, *43*, 3577.
(32) Papkov, V. S.; Gerasimov, M. V.; Dubovik, I. I.; Sharma, S.; Dementiev, V. V.; Pannell, K. H. *Macromolecules* **2000**, *33*, 7107.
(33) Hong, S.; MacKnight, W. J.; Russell, T. P.; Gido, S. P. *Macromolecules* **2001**, *34*, 2876.
(34) (a) Wunderlich, B. *Macromolecular Physic*; Academic Press: New York, 1973; Vol. *I*. (b) Cheng, S. Z. D. *Phase Transitions in Polymers: The Role of Metastable States*; Elsevier: Amsterdam, 2008.
(35) Xu, J.; Bellas, V.; Jungnickel, B.; Stühn, B.; Rehahn, M. *Macromol. Chem. Phys.* **2010**, *211*, 1261.
(36) Lammertink, R. G. H.; Hempenius, M. A.; Manners, I.; Vancso, G. J. *Macromolecules* **1998**, *31*, 795.
(37) Schultz, J. M. *Polymer Crystallization. The Development of Crystalline Order in Thermoplastic Polymers*; Oxford University Press: New York, 2001.
(38) Du, Z.-X.; Xu, J.-T.; Fan, Z.-Q. *Macromol. Rapid Commun.* **2008**, *29*, 467.
(39) Mihut, A. M.; Chiche, A.; Drechsler, M.; Schmalz, H.; Di Cola, E.; Krausch, G.; Ballauff, M. *Soft Matter* **2009**, *5*, 208.
(40) Mihut, A. M.; Crassous, J. J.; Schmalz, H.; Ballauff, M. *Colloid Polym. Sci.* **2010**, *288*, 573.
(41) He, W. N.; Xu, J. T.; Du, B. Y.; Fan, Z. Q.; Wang, X. S. *Macromol. Chem. Phys.* **2010**, *211*, 1909.
(42) Xu, J.; Ma, Y.; Hu, W.; Rehahn, M.; Reiter, G. *Nat. Mater.* **2009**, *8*, 348.
(43) Ungar, G.; Putra, E. G. R.; de Silva, D. S. M.; Shcherbina, M. A.; Waddon, A. J. *Adv. Polym. Sci.* **2005**, *180*, 45.
(44) Presa Soto, A.; Gilroy, J. B.; Winnik, M. A.; Manners, I. *Angew. Chem., Int. Ed.* **2010**, *49*, 8220.
(45) Eloi, J.-C.; Rider, D. A.; Cambridge, G.; Whittell, G. R.; Winnik, M. A.; Manners, I. *J. Am. Chem. Soc.* **2011**, *133*, 8903.
(46) Rupar, P. A.; Cambridge, G.; Winnik, M. A.; Manners, I. *J. Am. Chem. Soc.* **2011**, *133*, 16947.
(47) Ni, Y.; Rulkens, R.; Manners, I. *J. Am. Chem. Soc.* **1996**, *118*, 4102.